Quantum interference manipulation and enhancement with fluctuation-correlation-induced dephasing in an atomic system

Jinze Wu,[1] Jinhong Liu,[1] Yanyan He,[2] Yueying Zhang,[2] Junxiang Zhang,[1,2,*] and Shiyao Zhu[1,2]

[1]*State Key Laboratory of Quantum Optics and Quantum Optics Devices, Institute of Opto-Electronics, Shanxi University, Taiyuan 030006, China*

[2]*Department of Physics, Zhejiang University, Hangzhou 310027, China*

(Received 4 July 2018; published 15 October 2018)

We investigate the manipulation of the quantum interference (QI) in an electromagnetically induced transparency (EIT) system via phase fluctuations and their correlation of interacting fields. We show that the field fluctuation correlation and atomic dephasing rate have a similar effect to atomic coherence, and furthermore that QI is dependent on the fluctuation and correlation. Using the theoretical model in a dressed-state representation, the contribution of QI and Autler-Townes splitting (ATS) to probe absorption can be expressed in separate terms, such that the obvious enhancement of QI is found with highly correlated fields while ATS remains unchanged. In particular, when the relative large Rabi frequency of coupling field is applied, in which case the ATS plays a more prominent role than QI, we can still modulate the QI to be higher than ATS with correlated fields. This result could allow the strict EIT condition to be relaxed and be easily realized, or it may be a method to get a narrow EIT window for applications in efficient light storage and quantum interface.

DOI: 10.1103/PhysRevA.98.043829

I. INTRODUCTION

Electromagnetically induced transparency (EIT) [1–3] is a phenomenon in which a deep transparent window appears within a probe absorption spectrum with a linewidth even narrower than the natural linewidth [4], and thus it leads to extremely steep dispersion. EIT has been studied extensively for many years due to its wide applications in the slowing of light [5–8], optical storage [9–11], optical diodes [12], quantum communication [13,14], and quantum computation [15]. Experimental and theoretical studies showed that EIT can be used to enhance the nonlinear processes in atomic systems [16,17], and the combination of EIT and four-wave mixing (FWM) is a crucial way to generate narrowband biphotons [18–20] and continuous-variable correlated twin beams at the atomic transition wavelength [21–23], which are important resources in quantum communication networks [24].

In general, the transparent window is a joint effect of Autler-Townes splitting (ATS) [25,26] and quantum interference (QI) in three-level atomic systems. ATS originates from the dynamic Stark shifts of the two dressed states due to the coupling field. QI between the two transitions from the two dressed states to the ground state substantially deepens and narrows the transparent window. When the Rabi frequency of the coupling field is weaker than the decay rates, the two dressed states are so close to each other that they can be coupled to the same vacuum modes [27,28]. In this case, QI play a crucial role while the effect of ATS can be ignored. However, when the Rabi frequency of the coupling field is much stronger than the decay rates, the two dressed states are well separated, resulting in a negligible QI and an obvious ATS. Therefore, the Rabi frequency of the coupling field is responsible for the discrimination and identification of the QI and the ATS [29–32]. An objective method based on Akaike's information criterion (AIC) was proposed to discriminate EIT and ATS from experimental data [29–31], and it has been employed widely to quantitatively determine the relative weights of the effects of EIT and ATS in various systems [33–38].

Additionally, the nature of QI in the control of absorption via coupling fields was investigated for various atomic schemes, showing that QI can be manifested through two dispersive terms [39]. The narrow transparent window in an EIT medium is actually a result of destructive QI. Theoretical analysis showed that QI can be either destructive or constructive by changing the dephasing rates, leading to a reduction or enhancement of absorption [39,40]. In atomic media, it is well known that the dephasing is caused by the atom-atom and atom-environment collisions, which are difficult to precisely control in experiments.

In this article, we investigate the manipulation of the nature and strength of QI in a three-level atomic system via controlling the phase fluctuations and correlation of the coupling and probe fields. We show that the effect of the phase fluctuations and correlation is to induce another type of dephasing. This kind of dephasing, termed field-fluctuation induced dephasing (FFID), can be controlled flexibly and precisely by the phase modulation and locking techniques in experiments. We calculate the probe absorption that is a summation of an ATS term and a QI term in a dressed-state representation, showing that QI is associated with not only the Rabi frequency of the coupling field but also the dephasing

*Author to whom all correspondence should be addressed: junxiang_zhang@zju.edu.cn

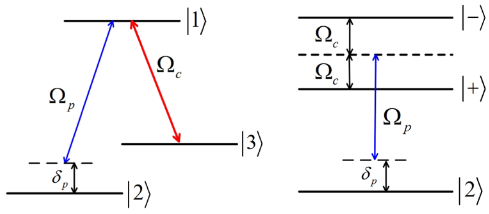

FIG. 1. (a) Λ-type three-level system. (b) Dressed-state representation.

rates. The dependence of QI on FFID and the Rabi frequency of the coupling field is analyzed in detail. In particular, the phase correlation between the coupling and the probe fields is shown to be a key factor to enhance QI.

II. FIELD-FLUCTUATION INDUCED DEPHASING

Consider the Λ-type three-level atomic system as shown in Fig. 1(a), consisting of an excited state, a ground state, and a metastable state, for example $|1\rangle = |6P_{1/2}, F = 4\rangle$, $|2\rangle = |6S_{1/2}, F = 3\rangle$, and $|3\rangle = |6S_{1/2}, F = 4\rangle$ in the D1 line of ^{133}Cs. The spontaneous decay rate from $|i\rangle$ to $|j\rangle$ $(i, j = 1, 2, 3)$ is represented by γ_{ij}, and the decoherence rate between $|i\rangle$ and $|j\rangle$ is Γ_{ij}. $\Gamma_{12} = (\gamma_{12} + \gamma_{13})/2 + \gamma_1^{(d)}$, $\Gamma_{13} = (\gamma_{12} + \gamma_{13})/2 + \gamma_1^{(d)} + \gamma_3^{(d)}$, and $\Gamma_{23} = \gamma_3^{(d)}$. $\gamma_1^{(d)}$ and $\gamma_3^{(d)}$ are the collisional dephasing rates, which are generally caused by the collisions among atoms. $\gamma_{12} = \gamma_{13} = 2.3$ MHz, $\gamma_1^{(d)} \approx \gamma_3^{(d)} \approx 0$, $\Gamma_{12} = \Gamma_{13} = 2.3$ MHz, and $\Gamma_{23} \approx 0$ for ^{133}Cs atoms. The frequency difference between the states $|i\rangle$ and $|j\rangle$ is $\omega_{ij} = \omega_i - \omega_j$. A strong-coupling field $E_c(t) = \mathcal{E}_c e^{-i[\nu_c t + \varphi_c(t)]} +$ c.c. drives the transition $|1\rangle \leftrightarrow |3\rangle$ resonantly, while a weak probe field $E_p(t) = \mathcal{E}_p e^{-i[\nu_p t + \varphi_p(t)]} +$ c.c. scans across the transition $|1\rangle \leftrightarrow |2\rangle$ with detuning $\delta_p = \omega_{12} - \nu_p$. Here the field fluctuations are taken into account by introducing the time-dependent random phases $\varphi_c(t)$ and $\varphi_p(t)$, while $\mathcal{E}_c$ and $\mathcal{E}_p$ are deterministic variables. The equations of density matrix elements are

$$\dot{\rho}_{22} = \gamma_{12}\rho_{11} - i\Omega_p e^{-i\varphi_p(t)}\rho_{21} + i\Omega_p e^{i\varphi_p(t)}\rho_{12}, \tag{1a}$$

$$\dot{\rho}_{33} = \gamma_{13}\rho_{11} - i\Omega_c e^{-i\varphi_c(t)}\rho_{31} + i\Omega_c e^{i\varphi_c(t)}\rho_{13}, \tag{1b}$$

$$\dot{\rho}_{12} = -(\Gamma_{12} + i\delta_p)\rho_{12} + i\Omega_c e^{-i\varphi_c(t)}\rho_{32} - i\Omega_p e^{-i\varphi_p(t)}(\rho_{11} - \rho_{22}), \tag{1c}$$

$$\dot{\rho}_{13} = -\Gamma_{13}\rho_{13} + i\Omega_p e^{-i\varphi_p(t)}\rho_{23} - i\Omega_c e^{-i\varphi_c(t)}(\rho_{11} - \rho_{33}), \tag{1d}$$

$$\dot{\rho}_{23} = -(\Gamma_{23} - i\delta_p)\rho_{23} - i\Omega_c e^{-i\varphi_c(t)}\rho_{21} + i\Omega_p e^{i\varphi_p(t)}\rho_{13}, \tag{1e}$$

where $\Omega_c = d_{13}\mathcal{E}_c/\hbar$ and $\Omega_p = d_{12}\mathcal{E}_p/\hbar$ are the Rabi frequencies of the coupling and probe fields, respectively, and they are assumed to be real. d_{ij} is the dipole moment of the transition $|i\rangle \leftrightarrow |j\rangle$. The phases $\varphi_c(t)$ and $\varphi_p(t)$ undergo diffusion: $\dot{\varphi}_c(t) = \mu_c(t)$ and $\dot{\varphi}_p(t) = \mu_p(t)$. $\varphi_c(0)$ and $\varphi_p(0)$ are uniformly distributed between 0 and 2π, and $\mu_c(t)$ and $\mu_p(t)$ are δ-correlated Gaussian random processes with [41,42]

$$\langle \mu_c(t)\rangle = \langle \mu_p(t)\rangle = 0, \tag{2a}$$

$$\langle \mu_c(t_1)\mu_c(t_2)\rangle = 2\kappa_c\delta(t_1 - t_2), \tag{2b}$$

$$\langle \mu_p(t_1)\mu_p(t_2)\rangle = 2\kappa_p\delta(t_1 - t_2), \tag{2c}$$

$$\langle \mu_c(t_1)\mu_p(t_2)\rangle = 2\kappa_{cp}\delta(t_1 - t_2). \tag{2d}$$

Here the angular brackets denote the ensemble average with respect to the distribution of random process $\mu_p(t)$ or $\mu_c(t)$. $2\kappa_c$ and $2\kappa_p$ represent the linewidths of the coupling and probe fields, respectively, and κ_{cp} is the cross-correlation coefficient of phase fluctuations between them. $\kappa_{cp} > 0$ $(\kappa_{cp} < 0)$ means phase correlation (anticorrelation) between the coupling and probe fields. If, for instance, the two fields are provided by two independent lasers, one has $\kappa_{cp} = 0$. The cross-correlation coefficient κ_{cp} varies in the range $[-\sqrt{\kappa_c\kappa_p}, \sqrt{\kappa_c\kappa_p}]$. For a typical diode laser (for example, TOPTICA DL PRO) commonly used in experiments, the free-running linewidths $\kappa_{c,p} \sim 1$ MHz. The linewidth of the laser can be adjusted up to $\sim$100 MHz via modulating the driving current by a wideband white-noise generator. The correlation (anticorrelation) between the phases of the two lasers can be controlled, e.g., using an optical phase-locked loop.

Introducing the variables

$$\tilde{\rho}_{12} = \rho_{12}e^{i\varphi_p(t)}, \quad \tilde{\rho}_{21} = \tilde{\rho}_{12}^*, \quad \tilde{\rho}_{13} = \rho_{13}e^{i\varphi_c(t)},$$
$$\tilde{\rho}_{31} = \tilde{\rho}_{13}^*, \quad \tilde{\rho}_{23} = \rho_{23}e^{i[\varphi_c(t) - \varphi_p(t)]}, \quad \tilde{\rho}_{32} = \tilde{\rho}_{23}^*, \tag{3}$$

Eqs. (1) become

$$\dot{\rho}_{22} = \gamma_{12}\rho_{11} - i\Omega_p\tilde{\rho}_{21} + i\Omega_p\tilde{\rho}_{12}, \tag{4a}$$

$$\dot{\rho}_{33} = \gamma_{13}\rho_{11} - i\Omega_c\tilde{\rho}_{31} + i\Omega_c\tilde{\rho}_{13}, \tag{4b}$$

$$\dot{\tilde{\rho}}_{12} = -(\Gamma_{12} + i\delta_p)\tilde{\rho}_{12} + i\mu_p(t)\tilde{\rho}_{12} + i\Omega_c\tilde{\rho}_{32} - i\Omega_p(\rho_{11} - \rho_{22}), \tag{4c}$$

$$\dot{\tilde{\rho}}_{13} = -\Gamma_{13}\tilde{\rho}_{13} + i\mu_c(t)\tilde{\rho}_{13} + i\Omega_p\tilde{\rho}_{23} - i\Omega_c(\rho_{11} - \rho_{33}), \tag{4d}$$

$$\dot{\tilde{\rho}}_{23} = -(\Gamma_{23} - i\delta_p)\tilde{\rho}_{23} - i\mu_p(t)\tilde{\rho}_{23} + i\mu_c(t)\tilde{\rho}_{23} - i\Omega_c\tilde{\rho}_{21} + i\Omega_p\tilde{\rho}_{13}. \tag{4e}$$

Considering the normalization condition $\rho_{11} + \rho_{22} + \rho_{33} = 1$, Eqs. (4) can be written as

$$\dot{P}_i = \sum_j A_{ij}P_j + \sum_j B_{ij}(t)P_j + C_i, \tag{5}$$

where P_i, A_{ij}, B_{ij}, and C_i are

$$P = (\rho_{22},\ \rho_{33},\ \tilde{\rho}_{12},\ \tilde{\rho}_{21},\ \tilde{\rho}_{13},\ \tilde{\rho}_{31},\ \tilde{\rho}_{23},\ \tilde{\rho}_{32})^{\mathrm{T}}, \tag{6}$$

$$C = (\gamma_{12},\ \gamma_{13},\ -i\Omega_p,\ i\Omega_p,\ -i\Omega_c,\ i\Omega_c,\ 0,\ 0,)^{\mathrm{T}}, \tag{7}$$

$$A = \begin{pmatrix} -\gamma_{12} & -\gamma_{12} & i\Omega_p & -i\Omega_p & 0 & 0 & 0 & 0 \\ -\gamma_{13} & -\gamma_{13} & 0 & 0 & i\Omega_c & -i\Omega_c & 0 & 0 \\ 2i\Omega_p & i\Omega_p & -(\Gamma_{12}+i\delta_p) & 0 & 0 & 0 & 0 & i\Omega_c \\ -2i\Omega_p & -i\Omega_p & 0 & -(\Gamma_{12}-i\delta_p) & 0 & 0 & -i\Omega_c & 0 \\ i\Omega_c & 2i\Omega_c & 0 & 0 & -\Gamma_{13} & 0 & i\Omega_p & 0 \\ -i\Omega_c & -2i\Omega_c & 0 & 0 & 0 & -\Gamma_{13} & 0 & -i\Omega_p \\ 0 & 0 & 0 & -i\Omega_c & i\Omega_p & 0 & -(\Gamma_{23}-i\delta_p) & 0 \\ 0 & 0 & i\Omega_c & 0 & 0 & -i\Omega_p & 0 & -(\Gamma_{23}+i\delta_p) \end{pmatrix}, \tag{8}$$

$$B(t) = \mathrm{diag}(0,\ 0,\ i\mu_p(t),\ -i\mu_p(t),\ i\mu_c(t),\ -i\mu_c(t),\ -i\mu_p(t)+i\mu_c(t),\ i\mu_p(t)-i\mu_c(t)). \tag{9}$$

$B(t)$ satisfies $\langle B_{ij}(t)\rangle = 0$ and $\langle B_{ij}(t_1)B_{kl}(t_2)\rangle = 2Q_{ijkl}\delta(t_1-t_2)$ with Q_{ijkl} obtained using Eqs. (2).

The average of P_i over the distributions of φ_c and φ_p is

$$\begin{aligned}\langle \dot{P}_i\rangle &= \sum_j A_{ij}\langle P_j\rangle + \sum_{jk} Q_{ikkj}\langle P_j\rangle + C_i \\ &= \sum_j A_{ij}\langle P_j\rangle + Q_{iiii}\langle P_i\rangle + C_i,\end{aligned} \tag{10}$$

where we have used the fact that Q_{ijkl} does not vanish only when $i=j$ and $k=l$ since $B(t)$ is a diagonal matrix. From Eqs. (2) and (9), we have

$$\begin{aligned} &Q_{3333} = Q_{4444} = -\kappa_p,\ Q_{5555} = Q_{6666} = -\kappa_c, \\ &Q_{7777} = Q_{8888} = -\kappa_p - \kappa_c + 2\kappa_{cp}. \end{aligned} \tag{11}$$

The equations of the mean density matrix elements are then

$$\langle \dot{\rho}_{22}\rangle = \gamma_{12}\langle\rho_{11}\rangle - i\Omega_p\langle\tilde{\rho}_{21}\rangle + i\Omega_p\langle\tilde{\rho}_{12}\rangle, \tag{12a}$$

$$\langle \dot{\rho}_{33}\rangle = \gamma_{13}\langle\rho_{11}\rangle - i\Omega_c\langle\tilde{\rho}_{31}\rangle + i\Omega_c\langle\tilde{\rho}_{13}\rangle, \tag{12b}$$

$$\langle \dot{\tilde{\rho}}_{12}\rangle = -(\tilde{\Gamma}_{12}+i\delta_p)\langle\tilde{\rho}_{12}\rangle + i\Omega_c\langle\tilde{\rho}_{32}\rangle - i\Omega_p(\langle\rho_{11}\rangle - \langle\rho_{22}\rangle), \tag{12c}$$

$$\langle \dot{\tilde{\rho}}_{13}\rangle = -\tilde{\Gamma}_{13}\langle\tilde{\rho}_{13}\rangle + i\Omega_p\langle\tilde{\rho}_{23}\rangle - i\Omega_c(\langle\rho_{11}\rangle - \langle\rho_{33}\rangle), \tag{12d}$$

$$\langle \dot{\tilde{\rho}}_{23}\rangle = -(\tilde{\Gamma}_{23}-i\delta_p)\langle\tilde{\rho}_{23}\rangle - i\Omega_c\langle\tilde{\rho}_{21}\rangle + i\Omega_p\langle\tilde{\rho}_{13}\rangle, \tag{12e}$$

with the effective decoherence rates

$$\tilde{\Gamma}_{12} = (\gamma_{12}+\gamma_{13})/2 + \gamma_1^{(d)} + \kappa_p, \tag{13a}$$

$$\tilde{\Gamma}_{13} = (\gamma_{12}+\gamma_{13})/2 + \gamma_1^{(d)} + \gamma_3^{(d)} + \kappa_c, \tag{13b}$$

$$\tilde{\Gamma}_{23} = \gamma_3^{(d)} + \kappa_c + \kappa_p - 2\kappa_{cp}. \tag{13c}$$

Equations (12) and (13) specifically show that the phase fluctuations and the correlation of the coupling and probe fields (i.e., the linewidths and the cross-correlation coefficient of the fields) have a similar effect to collisional dephasing only on the off-diagonal elements of the density matrix. This means that the phase fluctuations of fields cause the effect on the off-diagonal coherence elements of the density matrix, e.g., the atomic coherence determined by ρ_{12} for the probe field. We refer to this effect as field-fluctuation induced dephasing (FFID) quantified by κ_c, κ_p, and κ_{cp}.

In general, the spontaneous decay rates γ_{12} and γ_{13} are only determined by the selected atoms and cannot be changed, and on the other hand, the collisional dephasing rates $\gamma_1^{(d)}$ and $\gamma_3^{(d)}$ can be changed by changing the pressure of the buffer gas filled in the atoms in a vapor cell [43,44]. However, it is difficult to get the exact values of the dephasing rates, and one cannot adjust $\gamma_1^{(d)}$ ($\gamma_3^{(d)}$) while keeping $\gamma_3^{(d)}$ ($\gamma_1^{(d)}$) unchanged. Instead, changing the linewidths and the cross-correlation coefficient of lasers is relatively easy and purposeful using phase modulations and locking techniques. In the following sections, we mainly discuss the effect of FFID on QI, therefore we set $\gamma_1^{(d)} = \gamma_3^{(d)} = 0$, and also $\gamma_{12} = \gamma_{13} = \gamma$ for normalization.

III. MANIPULATION OF QI VIA FFID

To demonstrate the manipulation of QI by FFID, we calculate the probe absorption of the atomic medium in the dressed-state representation $|\pm\rangle = (|1\rangle \pm |3\rangle)/\sqrt{2}$ [see Fig. 1(b)], which is determined by the susceptibility

$$\chi = \frac{Nd_{12}}{\epsilon_0\mathcal{E}_p}\frac{1}{\sqrt{2}}(\langle\tilde{\rho}_{+2}\rangle + \langle\tilde{\rho}_{-2}\rangle), \tag{14}$$

where N is the atomic number density and ϵ_0 is the permittivity of vacuum. $\langle\tilde{\rho}_{+2}\rangle$ and $\langle\tilde{\rho}_{-2}\rangle$ satisfy the equations

$$\begin{aligned}\langle\dot{\tilde{\rho}}_{+2}\rangle = &-[i(\delta_p-\Omega_c)+\xi]\langle\tilde{\rho}_{+2}\rangle - \eta\langle\tilde{\rho}_{-2}\rangle \\ &+ \frac{i\Omega_p}{\sqrt{2}}(\langle\rho_{22}\rangle - \langle\tilde{\rho}_{++}\rangle - \langle\tilde{\rho}_{+-}\rangle),\end{aligned} \tag{15a}$$

$$\begin{aligned}\langle\dot{\tilde{\rho}}_{-2}\rangle = &-[i(\delta_p+\Omega_c)+\xi]\langle\tilde{\rho}_{-2}\rangle - \eta\langle\tilde{\rho}_{+2}\rangle \\ &+ \frac{i\Omega_p}{\sqrt{2}}(\langle\rho_{22}\rangle - \langle\tilde{\rho}_{--}\rangle - \langle\tilde{\rho}_{-+}\rangle),\end{aligned} \tag{15b}$$

with

$$\xi = (\tilde{\Gamma}_{12}+\tilde{\Gamma}_{23})/2 = \gamma/2 + (\kappa_c + 2\kappa_p - 2\kappa_{cp})/2, \tag{16a}$$

$$\eta = (\tilde{\Gamma}_{12}-\tilde{\Gamma}_{23})/2 = \gamma/2 + (2\kappa_{cp} - \kappa_c)/2. \tag{16b}$$

ξ and η are the parameters characterized by the spontaneous decay rate of atoms, the phase fluctuations of the coupling and probe fields, and phase correlation of the fields.

Considering that the probe field is much weaker than the coupling field, and keeping the probe field only up to the first order and the coupling field up to all orders, we obtain the mean density matrix elements $\langle\tilde{\rho}_{+2}\rangle$ and $\langle\tilde{\rho}_{-2}\rangle$ in a dressed-state representation:

$$\langle \tilde{\rho}_{+2} \rangle = \frac{i\Omega_p}{\sqrt{2}} \frac{i(\delta_p + \Omega_c) + \xi - \eta}{[i(\delta_p - \Omega_c) + \xi][i(\delta_p + \Omega_c) + \xi] - \eta^2}, \tag{17a}$$

$$\langle \tilde{\rho}_{-2} \rangle = \frac{i\Omega_p}{\sqrt{2}} \frac{i(\delta_p - \Omega_c) + \xi - \eta}{[i(\delta_p - \Omega_c) + \xi][i(\delta_p + \Omega_c) + \xi] - \eta^2}. \tag{17b}$$

The absorption of the probe field is then obtained,

$$\mathrm{Im}\chi \propto \frac{\xi}{(\delta_p - \Omega_c)^2 + \xi^2} + \frac{\xi}{(\delta_p + \Omega_c)^2 + \xi^2} + \Phi. \tag{18}$$

The first two terms of Eq. (18) are two Lorentzian absorption profiles with the same linewidth ξ and splitting width $2\Omega_c$. The third term is expressed as

$$\Phi = -\mathrm{Re}\frac{2\eta\left[(i\delta_p + \xi)(i\delta_p + \xi - \eta) + \Omega_c^2\right]}{\left[(i\delta_p + \xi)^2 + \Omega_c^2\right]\left[(i\delta_p + \xi)^2 - \eta^2 + \Omega_c^2\right]}. \tag{19}$$

It can be seen from Eqs. (15), (18), and (19) that η determines the quantum interference between the transitions $|+\rangle \leftrightarrow |2\rangle$ and $|-\rangle \leftrightarrow |2\rangle$. If $\eta = 0$, we have $\Phi = 0$, and Eqs. (15a) and (15b) reduce to two independent equations, meaning that the transitions $|+\rangle \leftrightarrow |2\rangle$ and $|-\rangle \leftrightarrow |2\rangle$ are independent without interference. As a result, the absorption is simply the superposition of the first two terms of Eq. (18), characterized as ATS [45]. This effect can be understood from the Λ-type EIT system in Fig. 1(a), in which EIT is obtained under the condition that the spontaneous decay rates γ_{12} and γ_{13} from the excited state $|1\rangle$ to the ground states $|2\rangle$ and $|3\rangle$ are much larger than the nonradiative decay rate γ_{23} between the states $|2\rangle$ and $|3\rangle$, i.e., γ_{12} $(\gamma_{13}) \gg \gamma_{23}$. In this case, $\eta = (\gamma_{12} + \gamma_{13})/4 - \gamma_{23}/2 > 0$. Any increase of the nonradiative decay rate γ_{23} (i.e., $\eta = \gamma/2 - \gamma_{23}/2 \sim 0$, e.g., due to large collisional dephasing in atoms) will reduce the EIT effect. On the other hand, Eq. (16b) also shows that the phase fluctuation κ_c has a similar effect on EIT as γ_{23}, while the phase correlation κ_{cp} can compensate for this reduction.

The third term Φ of Eq. (18) is the contribution of QI between the two transitions in the absorption spectrum. If $\Phi < 0$ $(\Phi > 0)$, the absorption is suppressed (enhanced) relative to the case of ATS $(\Phi = 0)$, which is referred to as destructive (constructive) QI. A large (small) $|\Phi|$ indicates that QI has a strong (weak) effect on the absorption. It is therefore concluded that the nature of QI is determined by the sign of Φ while the strength of the effect of QI is represented by $|\Phi|$.

Next, we analyze the effect of FFID on Φ at $\delta_p = 0$ (for the case of resonance of the probe field), denoted as

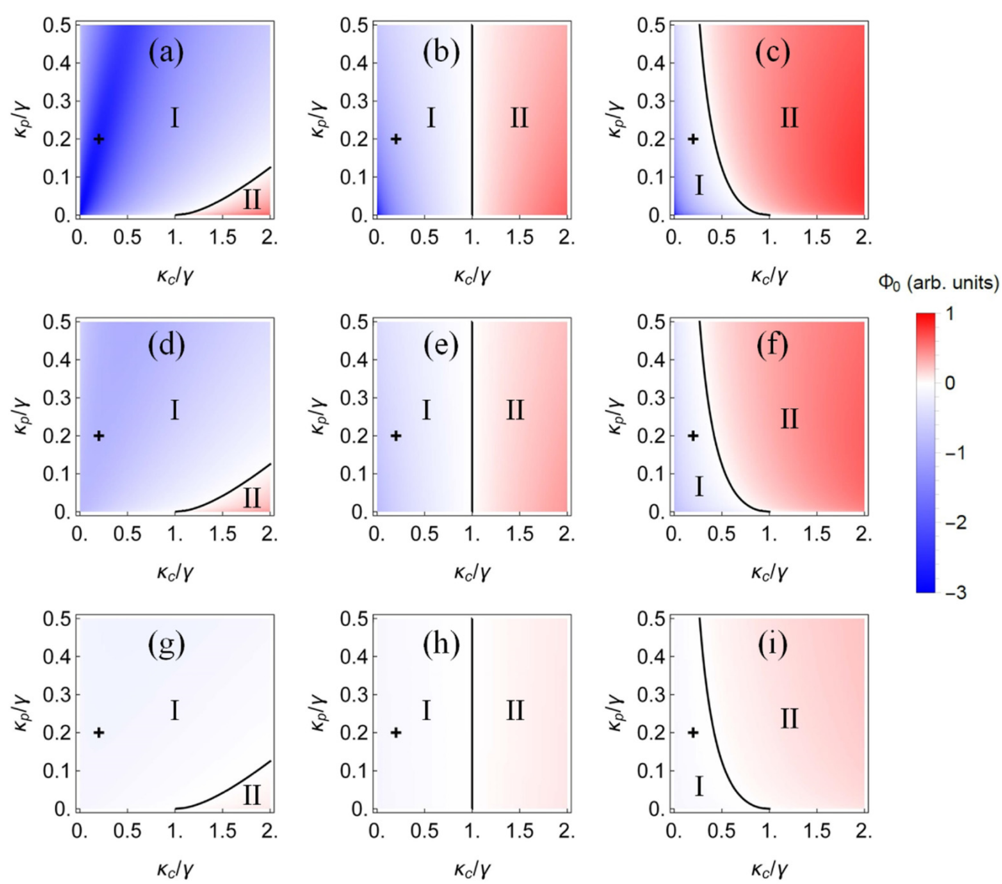

FIG. 2. Φ_0 vs κ_c and κ_p for $\kappa_{cp} = \sqrt{\kappa_c \kappa_p}$ (first column), $\kappa_{cp} = 0$ (second column), and $\kappa_{cp} = -\sqrt{\kappa_c \kappa_p}$ (third column) with $\Omega_c = 0.3\gamma$ (first row), $\Omega_c = \gamma$ (second row), and $\Omega_c = 3\gamma$ (third row). The regions I, the regions II, and the black lines indicate $\Phi_0 < 0$ (destructive QI), $\Phi_0 > 0$ (constructive QI), and $\Phi_0 = 0$ (no QI), respectively. The cross marks indicate the general EIT experiment condition, i.e., $\kappa_c = \kappa_p = 0.2\gamma$ (linewidths of $\sim$1 MHz).

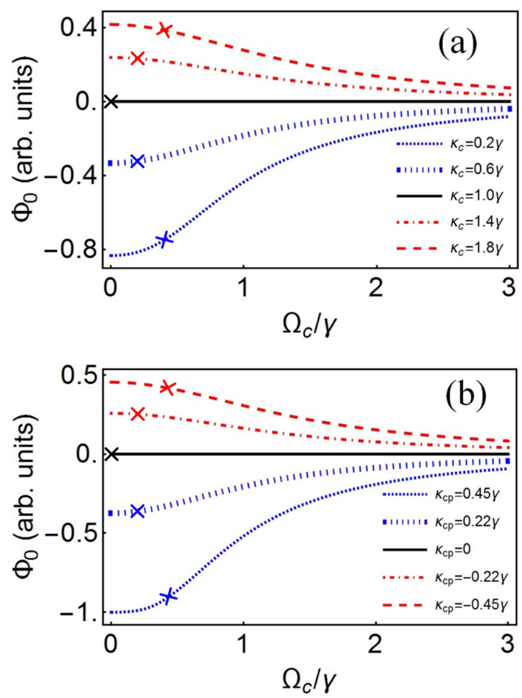

FIG. 3. Φ_0 vs Ω_c (a) for different κ_c with $\kappa_p = 0.2\gamma$ and $\kappa_{cp} = 0$; (b) for different κ_{cp} with $\kappa_c = \gamma$ and $\kappa_p = 0.2\gamma$. The cross marks indicate $\Omega_c = \Omega_{\text{th}} = |\eta|$.

$\Phi_0 = -2\eta[\xi(\xi-\eta)+\Omega_c^2]/[(\xi^2+\Omega_c^2)(\xi^2-\eta^2+\Omega_c^2)]$. Figure 2 shows the dependence of Φ_0 on κ_c and κ_p for $\kappa_{cp} = \sqrt{\kappa_c\kappa_p}$ (the maximum phase correlation between the coupling and probe fields), $\kappa_{cp} = 0$ (no phase correlation), and $\kappa_{cp} = -\sqrt{\kappa_c\kappa_p}$ (the maximum phase anticorrelation), respectively. Regions I represent $\Phi_0 < 0$ (destructive QI, i.e., EIT) while regions II represent $\Phi_0 > 0$ (constructive QI). The black lines in each figure are boundaries of the two regions and indicate $\Phi_0 = 0$ (no QI). It can be seen from Fig. 2 that as κ_{cp} changes from $\sqrt{\kappa_c\kappa_p}$ to $-\sqrt{\kappa_c\kappa_p}$, the region of destructive QI (region I) becomes small, while the region of constructive QI (region II) becomes large, showing that the FFID gives rise to the manipulation of QI. One can improve the QI in atoms using phase-correlated fields. The cross marks in each figure of Fig. 2 show the case for the general EIT experiment with two separate coupling and probe fields (the linewidth is ~1 MHz, i.e., $\kappa_c = \kappa_p = 0.2\gamma$). It is seen that QI is always destructive ($\Phi_0 < 0$) in EIT experiments, and the EIT can be enhanced (Φ_0 decreases) using phase-correlated fields via the phase-locking technique ($\kappa_{cp} > 0$).

Φ_0 depends not only on κ_c, κ_p, and κ_{cp}, but also on Ω_c [see Eq. (19)]. It is seen from Fig. 2 that the effect of QI becomes weaker for larger Ω_c. In Fig. 3, we plot Φ_0 as a function of Ω_c. Φ_0 tends to zero as Ω_c increases, implying that the effect of QI becomes negligible. Actually, it can be easily verified that $\lim_{\Omega_c\to\infty}\Phi_0 = 0$ regardless of the values of κ_c, κ_p, and κ_{cp}. This fact can be understood straightforwardly in the dressed-state representation [see Fig. 1(b)] where the splitting between the two dressed states $|\pm\rangle$ is $2\Omega_c$. For a small Ω_c, $|\pm\rangle$ are close to each other and can be coupled to the ground state $|2\rangle$ by the same vacuum modes [27,28], leading to strong QI between the two transitions $|+\rangle \leftrightarrow |2\rangle$ and $|-\rangle \leftrightarrow |2\rangle$. On the other hand, for a large Ω_c, $|\pm\rangle$ are well separated and can only be coupled to $|2\rangle$ by different vacuum modes, implying that the effect of QI is negligible and the absorption is mainly due to the effect of ATS.

Actually, the total absorption in Eq. (18) is determined by the first two Lorentzian terms (characterized as ATS) and QI terms of Φ. The relative weights of QI and ATS are the key evidence to see which one is important. It is obvious in Figs. 2 and 3 that Ω_c is one factor to determine the weight of QI, and is characterized by a threshold $\Omega_{\text{th}} = |\eta|$ as discussed in Refs. [29–31]. When $\Omega_{\text{th}} < |\eta|$, the effect of QI is prominent while the effect of ATS is negligible. When $\Omega_{\text{th}} \gg |\eta|$, the effect of ATS dominates while the effect of EIT can be

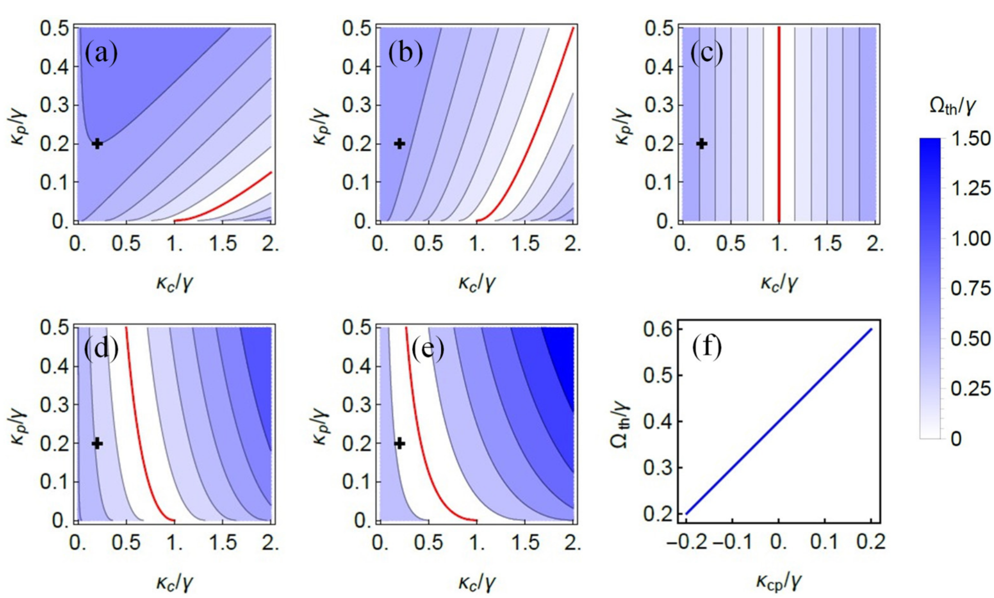

FIG. 4. Ω_{th} vs κ_c and κ_p for (a) $\kappa_{cp} = \sqrt{\kappa_c\kappa_p}$, (b) $\kappa_{cp} = \sqrt{\kappa_c\kappa_p}/2$, (c) $\kappa_{cp} = 0$, (d) $\kappa_{cp} = -\sqrt{\kappa_c\kappa_p}/2$, and (e) $\kappa_{cp} = -\sqrt{\kappa_c\kappa_p}$. The red lines indicate $\Omega_{\text{th}} = 0$. The cross marks indicate the general EIT experiment condition, i.e., $\kappa_c = \kappa_p = 0.2\gamma$ (linewidths of ~1 MHz). Ω_{th} vs κ_{cp} for this condition is plotted in (f).

ignored. For a moderate value of Ω_c, both effects of EIT and ATS are important. In our study, the threshold Ω_{th} can be manipulated by FFID. Figure 4 shows the dependence of Ω_{th} on κ_c and κ_p for different κ_{cp}. Ω_{th} is intensely modulated by κ_c, κ_p, and κ_{cp}, and can be enlarged. In this case, it is possible to get prominent QI for larger Ω_c. For example, when $\kappa_c = \gamma$ and $\kappa_{cp} = 0$ [see Fig. 4(c)], $\Omega_{\text{th}} = 0$ for any Ω_c. In Fig. 4(f), we plot Ω_{th} as a function of κ_{cp} with typical EIT experimental parameters $\kappa_c = \kappa_p = 0.2\gamma$ [also cross marks in Figs. 4(a)–4(e)]. In a typical experiment, $\kappa_{cp} = 0$ and $\Omega_{\text{th}} = 0.4\gamma$ (0.92 MHz for ^{133}Cs D1 line) thus the effect of EIT dominates when $\Omega_{\text{th}} < 0.4\gamma$. As κ_{cp} increases to its maximum value 0.2γ, Ω_{th} increases up to 0.6γ (1.38 MHz for the ^{133}Cs D1 line), implying that the effect of EIT is prominent in a wider range, i.e., $\Omega_c < 0.6\gamma$.

IV. CONCLUSION

In conclusion, we studied the quantum interference effects induced by the phase fluctuations and their correlation of the fields in a Λ-type EIT system. By calculating the probe absorption in the dressed-state representation, we got the two separated terms for Autler-Townes splitting and quantum interference effects, respectively. The quantum interference and the relative weights of Autler-Townes splitting and quantum interference can be manipulated flexibly by field phase fluctuations and the correlation. In particular, the weight of quantum interference can be enhanced under the condition of a larger Rabi frequency of a coupling field. This makes the EIT effect easily obtained or enhanced under normal conditions.

ACKNOWLEDGMENTS

This work was supported by National Natural Science Foundation of China (91736209, U1330203, and 11574188); National Natural Science Foundation of China (11634008), and Zhejiang Provincial Natural Science Foundation of China under Grant No. LD18A040001.

[1] K.-J. Boller, A. Imamoğlu, and S. E. Harris, Observation of Electromagnetically Induced Transparency, Phys. Rev. Lett. **66**, 2593 (1991).

[2] M. Fleischhauer, A. Imamoglu, and J. P. Marangos, Electromagnetically induced transparency: Optics in coherent media, Rev. Mod. Phys. **77**, 633 (2005).

[3] S. E. Harris, Electromagnetically induced transparency, Phys. Today **50**(7), 36 (1997).

[4] S. M. Iftiquar, G. R. Karve, and V. Natarajan, Subnatural linewidth for probe absorption in an electromagnetically-induced-transparency medium due to Doppler averaging, Phys. Rev. A **77**, 063807 (2008).

[5] L. V. Hau, S. E. Harris, Z. Dutton, and C. H. Behroozi, Light speed reduction to 17 metres per second in an ultracold atomic gas, Nature (London) **397**, 594 (1999).

[6] S. Raza and S. I. Bozhevolnyi, Slow-light plasmonic metamaterial based on dressed-state analog of electromagnetically induced transparency, Opt. Lett. **40**, 4253 (2015).

[7] R. Liu, T. Liu, Y. Wang, Y. Li, and B. Gai, Slowing down the speed of light using an electromagnetically-induced-transparency mechanism in a modified reservoir, Phys. Rev. A **96**, 053823 (2017).

[8] Z. Wu, R.-H. Luo, J.-Q. Zhang, Y.-H. Wang, W. Yang, and M. Feng, Force-induced transparency and conversion between slow and fast light in optomechanics, Phys. Rev. A **96**, 033832 (2017).

[9] D. F. Phillips, A. Fleischhauer, A. Mair, R. L. Walsworth, and M. D. Lukin, Storage of Light in Atomic Vapor, Phys. Rev. Lett. **86**, 783 (2001).

[10] G. Heinze, C. Hubrich, and T. Halfmann, Stopped Light and Image Storage by Electromagnetically Induced Transparency up to the Regime of One Minute, Phys. Rev. Lett. **111**, 033601 (2013).

[11] Y. O. Dudin, L. Li, and A. Kuzmich, Light storage on the time scale of a minute, Phys. Rev. A **87**, 031801(R) (2013).

[12] D.-W. Wang, H.-T. Zhou, M.-J. Guo, J.-X. Zhang, J. Evers, and S.-Y. Zhu, Optical Diode Made from a Moving Photonic Crystal, Phys. Rev. Lett. **110**, 093901 (2013).

[13] M. D. Lukin, Colloquium: Trapping and manipulating photon states in atomic ensembles, Rev. Mod. Phys. **75**, 457 (2003).

[14] K. Hammerer, A. S. Sørenssen, and E. S. Polzik, Quantum interface between light and atomic ensembles, Rev. Mod. Phys. **82**, 1041 (2010).

[15] E. Knill, R. Laflamme, and G. J. Milburn, A scheme for efficient quantum computation with linear optics, Nature (London) **409**, 46 (2001).

[16] D. A. Braje, V. Balić, S. Goda, G. Y. Yin, and S. E. Harris, Frequency Mixing Using Electromagnetically Induced Transparency in Cold Atoms, Phys. Rev. Lett. **93**, 183601 (2004).

[17] C.-Y. Lee, B.-H. Wu, G. Wang, Y.-F. Chen, Y.-C. Chen, and I. A. Yu, High conversion efficiency in resonant four-wave mixing processes, Opt. Express **24**, 1008 (2016).

[18] L. Zhao, Y. Su, and S. Du, Narrowband biphoton generation in the group delay regime, Phys. Rev. A **93**, 033815 (2016).

[19] C. Shu, P. Chen, T. K. A. Chow, L. Zhu, Y. Xiao, M. M. T. Loy, and S. Du, Subnatural-linewidth biphotons from a Doppler-broadened hot atomic vapour cell, Nat. Commun. **7**, 12783 (2016).

[20] L. Zhu, X. Guo, C. Shu, H. Jeong, and S. Du, Bright narrowband biphoton generation from a hot rubidium atomic vapor cell, Appl. Phys. Lett. **110**, 161101 (2017).

[21] T. T. Grove, M. S. Shahriar, P. R. Hemmer, P. Kumar, V. S. Sudarshanam, and M. Cronin-Golomb, Distortion-free gain and noise correlation in sodium vapor with four-wave mixing and coherent population trapping, Opt. Lett. **22**, 769 (1997).

[22] C. F. McCormick, V. Boyer, E. Arimondo, and P. D. Lett, Strong relative intensity squeezing by four-wave mixing in rubidium vapor, Opt. Lett. **32**, 178 (2007).

[23] M.-J. Guo, H.-T. Zhou, D. Wang, J.-R. Gao, J.-X Zhang, and S.-Y. Zhu, Experimental investigation of high-frequency-

difference twin beams in hot cesium atoms, Phys. Rev. A **89**, 033813 (2014).

[24] L.-M. Duan, M. D. Lukin, J. I. Cirac, and P. Zoller, Long-distance quantum communication with atomic ensembles and linear optics, Nature (London) **414**, 413 (2001).

[25] S. H. Autler and C. H. Townes, Stark effect in rapidly varying fields, Phys. Rev. **100**, 703 (1955).

[26] C. N. Cohen-Tannoudji, The Autler-Townes effect revisited, in *Amazing light*, edited by R. Y. Chiao (Springer, New York, 1996).

[27] S.-Y. Zhu, R. C. F. Chan, and C. P. Lee, Spontaneous emission from a three-level atom, Phys. Rev. A **52**, 710 (1995).

[28] S.-Y. Zhu, L. M. Narducci, and M. O. Scully, Quantum-mechanical interference effects in the spontaneous-emission spectrum of a driven atom, Phys. Rev. A **52**, 4791 (1995).

[29] P. M. Anisimov, J. P. Dowling, and B. C. Sanders, Objectively Discerning Autler-Townes Splitting from Electromagnetically Induced Transparency, Phys. Rev. Lett. **107**, 163604 (2011).

[30] L. Giner, L. Veissier, B. Sparkes, A. S. Sheremet, A. Nicolas, O. S. Mishina, M. Scherman, S. Burks, I. Shomroni, D. V. Kupriyanov, P. K. Lam, E. Giacobino, and J. Laurat, Experimental investigation of the transition between Autler-Townes splitting and electromagnetically-induced-transparency models, Phys. Rev. A **87**, 013823 (2013).

[31] P. Anisimov and O. Kocharovskaya, Decaying-dressed-state analysis of a coherently driven three-level Λ system, J. Mod. Opt. **55**, 3159 (2008).

[32] T. Y. Abi-Salloum, Electromagnetically induced transparency and Autler-Townes splitting: Two similar but distinct phenomena in two categories of three-level atomic systems, Phys. Rev. A **81**, 053836 (2010).

[33] B. Peng, Ş. K. Özdemir, W. Chen, F. Nori, and L. Yang, What is and what is not electromagnetically induced transparency in whispering-gallery microcavities, Nat. Commun. **5**, 5082 (2014).

[34] C.-J. Zhu, C.-H. Tan, and G.-X. Huang, Crossover from electromagnetically induced transparency to Autler-Townes splitting in open V-type molecular systems, Phys. Rev. A **87**, 043813 (2013).

[35] H.-C. Sun, Y.-X. Liu, H. Ian, J. Q. You, E. Il'ichev, and F. Nori, Electromagnetically induced transparency and Autler-Townes splitting in superconducting flux quantum circuits, Phys. Rev. A **89**, 063822 (2014).

[36] Q.-C. Liu, T.-F. Li, X.-Q. Luo, H. Zhao, W. Xiong, Y.-S. Zhang, Z. Chen, J. S. Liu, W. Chen, F. Nori, J. S. Tsai, and J. Q. You, Method for identifying electromagnetically induced transparency in a tunable circuit quantum electrodynamics system, Phys. Rev. A **93**, 053838 (2016).

[37] H.-C. Li, G.-Q. Ge, and H.-Y. Zhang, Dressed-state realization of the transition from electromagnetically induced transparency to Autler-Townes splitting in superconducting circuits, Opt. Express **23**, 9844 (2015).

[38] L.-Y. He, T.-J. Wang, Y.-P. Gao, C. Cao, and C. Wang, Discerning electromagnetically induced transparency from Autler-Townes splitting in plasmonic waveguide and coupled resonators system, Opt. Express **23**, 23817 (2015).

[39] G. S. Agarwal, Nature of the quantum interference in electromagnetic-field-induced control of absorption, Phys. Rev. A **55**, 2467 (1997).

[40] S. Davuluri, Y.-P. Wang, and S.-Y. Zhu, Destructive and constructive interference in the coherently driven three-level systems, J. Mod. Opt. **62**, 1091 (2015).

[41] G. S. Agarwal, Quantum statistical theory of optical-resonance phenomena in fluctuating laser fields, Phys. Rev. A **18**, 1490 (1978).

[42] R. Saxena and G. S. Agarwal, Modulated Hanle signals in partially coherent fields, Phys. Rev. A **25**, 2123 (1982).

[43] E. E. Mikhailov, I. Novikova, Y. V. Rostovtsev, and G. R. Welch, Buffer-gas-induced absorption resonances in Rb vapor, Phys. Rev. A **70**, 033806 (2004).

[44] A. Sargsyan, D. Sarkisyan, U. Krohn, J. Keaveney, and C. Adams, Effect of buffer gas on an electromagnetically induced transparency in a ladder system using thermal rubidium vapor, Phys. Rev. A **82**, 045806 (2010).

[45] C. Cohen-Tannoudji, J. Dupont-Roc, and G. Grynberg, *Atom-Photon Interactions: Basic Processes and Applications* (Wiley Interscience, New York, 1998).